Distinct-symmetry spin-liquid states and phase diagram of the Kitaev-Hubbard model

Long Liang, Ziqiang Wang, and Yue Yu

Symmetry distinct spin liquid states and phase diagram of Kitaev-Hubbard model

Long Liang[1], Ziqiang Wang[2], and Yue Yu[3,1]

[1]State Key Laboratory of Theoretical Physics, Institute of Theoretical Physics,
Chinese Academy of Sciences, P.O. Box 2735, Beijing 100190, China
[2] Department of Physics, Boston College, Chestnut Hill, Massachusetts 02467, USA
[3]Department of Physics, Center for Field Theory and Particle Physics,
and State Key Laboratory of Surface Physics, Fudan University, Shanghai 200433, China

We report the finding of a series of symmetry distinct spin liquid (SL) states and a rich phase diagram in a half-filled honeycomb lattice Hubbard model with spin-dependent hopping amplitude t'. We first study the magnetic instability of the system and find two antiferromagnetic (AF) orders beyond a critical Hubbard U which increases with the ratio t'/t. For t' approaching to t, the semimetal (SM) transforms to a $U(1)$ SL and then to the Kitaev Z_2 SL as U increases. In a wide middle range of t'/t, the latter is replaced by a $U(1)$ SL to $SU(2)$ SL transition. The physical properties of the stable SL phases are discussed.

I. INTRODUCTION

Searching for the spin liquid (SL) states[1,2] in strongly correlated systems has been one of the most intriguing and important fields[3]. Experimentally, possible SL states have been observed recently in quantum frustrated spin systems[4–9]. Theoretically, ample numerical evidence of SL ground state has been found in models of frustrated spin systems[10–14] and various exactly solvable models have been constructed to support the existence of the SL ground state[15–20].

While most of the studies focused on quantum spin systems, possible SL states in the Hubbard model near the metal-insulator transition have attracted great interests recently. Quantum Monte Carlo studies have produced controversial results[21–23] amid an active debate over other investigations[24–31]. Whether a SL ground state exists remains inconclusive due to the intricate interplay of charge and spin dynamics in the quantum critical region of the metal insulator transition and the incipient antiferromagnetic (AF) order.

We here study the ground state and the phase diagram of a generalized $t - t' - U$ Hubbard model where t' describes nearest neighbor spin-dependent hopping on the half-filled honeycomb lattice. This model, which we call a Kitaev-Hubbard model, was introduced by Duan et al, and can be realized in cold atom systems[32–34], has been studied numerically at quarter filling[35] and half filling[36,37]. Our motivation is that as a function of t'/t, this model interpolates between the usual Hubbard model at $t'/t = 0$ and 1 where the Kitaev Z_2 SL[17,38] becomes the known ground state in the large on-site U limit[32,36,39]. With the latter severing as a reference SL state, we obtain a rich phase diagram on the $U/t - t'/t$ plane that reveals the phase structure of several symmetry distinct SL states on the honeycomb lattice as well as their competition with several forms of AF order.

A SL is a Mott insulator without spin order that has exotic charge-neutral excitations called spinons which are coupled by emerging gauge fields[40]. Most commonly studied SLs are $U(1)$, $SU(2)$, and Z_2 SL - named after the symmetry of the gauge fields, respectively. In this work, we show that these SL states emerge on the phase diagram of the Kitaev-Hubbard model at half filling and have yet to be explored by numerical studies[36]. Specifically, we apply the $SU(2)$ slave rotor theory[41,42] to the Kitaev-Hubbard model, which recovers the semimetal (SM) phase with stable Dirac points at weak interactions, and search for all possible SL phases with gapless fermionic spinon excitations coupled to the corresponding gauge groups. We also calculate the spin susceptibility using the random phase approximation (RPA) and determine the stability of the SLs against magnetic ordering on the honeycomb lattice. The physical characters of the different SLs that are experimentally distinguishable will be discussed.

The present paper is organized as follows. In section II we describe the model and its symmetries. We study the magnetic instabilities using RPA in section III. In section IV, we use $SU(2)$ slave rotor theory to study the SL phases. Then we describe how to combine the results of RPA and slave rotor to obtain the global phase diagram in section V. Finally, we discuss how to measure the different phases in cold atom experiments in section VI.

II. THE MODEL AND ITS SYMMETRIES

The Hamiltonian for the Kitaev-Hubbard model on a honeycomb lattice[32] is given by

$$H = -t \sum_{\langle ij \rangle} c_i^\dagger c_j - t' \sum_{\langle ij \rangle_a} c_i^\dagger \sigma^a c_j + U \sum_i n_{i\uparrow} n_{i\downarrow}, \quad (1)$$

where $c_i = [c_{i\uparrow}, c_{i\downarrow}]^T$ and $c_{i\sigma}$ ($c_{i\sigma}^\dagger$) annihilates (creates) an electron with spin $\sigma = (\uparrow, \downarrow)$ on site i. The t-term is the conventional hopping integral, while the t'-term describes link-and-spin-dependent hopping, and U is the on-site repulsion. σ^a ($a = x, y, z$) are the Pauli matrices. $\langle ij \rangle_a$ denotes the nearest neighbor pairs in the a-link direction(see Fig.1).
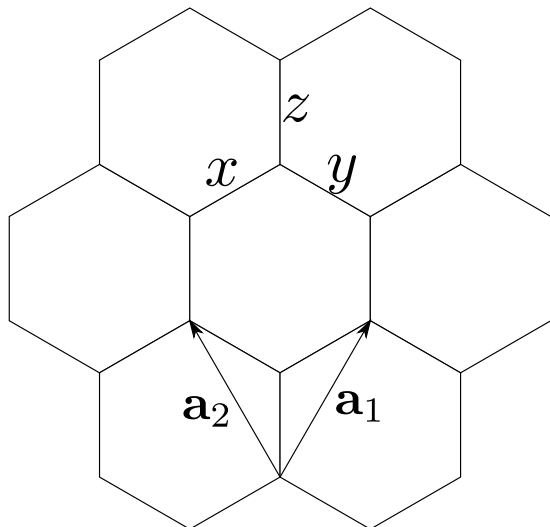
FIG. 1: Honeycomb lattice. $\mathbf{a}_1$ and $\mathbf{a}_2$ are primitive translation vectors. Nearest-neighbor links are divided into three types, called x-links, y-links and z-links.

We group the electron operators into 2×2 matrices[43]

$$\Psi_A = \begin{bmatrix} c_{A\uparrow} & c_{A\downarrow}^\dagger \\ c_{A\downarrow} & -c_{A\uparrow}^\dagger \end{bmatrix}, \quad \Psi_B = \begin{bmatrix} c_{B\uparrow} & -c_{B\downarrow}^\dagger \\ c_{B\downarrow} & c_{B\uparrow}^\dagger, \end{bmatrix} \quad (2)$$

where A and B label sites on the two sub-lattices, and define spin and pseudo-spin operators as

$$S^a = \frac{1}{4}\mathrm{Tr}(\Psi^\dagger \sigma^a \Psi), \ T^a = \frac{1}{4}\mathrm{Tr}(\Psi \sigma^a \Psi^\dagger)$$

S^a acts on the subspace with odd electron number while T^a acts on the subspace with even electron number so they are commutative with one another.

To reveal the symmetry it's convenient to rewrite the Hamiltonian in terms of Ψ_A and Ψ_B:

$$H = -t \sum_{\langle A,B\rangle} \mathrm{Tr}(\Psi_A^\dagger \Psi_B) - t' \sum_{\langle A,B\rangle_a} \mathrm{Tr}(\sigma^z \Psi_A^\dagger \sigma^a \Psi_B)$$
$$+ \frac{2U}{3}\sum_i \mathbf{T}_i^2. \quad (3)$$

The t-term clearly preserves spin and pseudo-spin rotational symmetries while the t'-term also preserves spin and pseudo-spin rotational symmetries if we perform suitable local rotation of Ψs. (See Appendix A.) However, when both t and t' are non-zero, both $SU(2)$ symmetries are broken since the symmetry operations of t-term and t'-term are not compatible with each other. There is an important discrete chiral symmetry associated with the operator: $\mathcal{S} = \mathcal{P} \cdot \mathcal{T}$ where $\mathcal{P} = e^{i\pi T^y}$ is particle-hole and $\mathcal{T} = e^{i\pi S^y} K$ the time-reversal operation(K is complex conjugation). Because of this symmetry, TRS is enforced at half-filling in the large U limit[36] as seen in the phase diagram in Fig.5. In

contrast to the usual lattice translation T_x and T_y and the inversion $\mathcal{R}$ symmetries that are preserved, the six-fold rotational symmetry is broken due to the t'-term. However, the system is invariant under combined $\pi/3$ lattice rotation and a spin rotation,

$$\Psi_{A,B} \to e^{-i\frac{\pi}{4}\sigma^x} e^{-i\frac{\pi}{4}\sigma^y} \Psi_{A,B}$$

In the noninteracting limit $(U = 0)$[34], the electron dispersion $\varepsilon(\mathbf{k})$ is given by

$$\varepsilon^2(\mathbf{k}) = t^2|f|^2 + 3t'^2 \pm [(t^2|f|^2 + 3t'^2)^2$$
$$- |t'^2(g_+g_- + 1) - t^2 f^2|^2]^{1/2}, \quad (4)$$

where $g_\pm = e^{ik_1} \pm ie^{ik_2}$ and $f(\mathbf{k}) = 1 + e^{ik_1} + e^{ik_2}$. $k_1 = \mathbf{k}\cdot\mathbf{a}_1 = k_x/2 + \frac{\sqrt{3}k_y}{2}$, $k_2 = \mathbf{k}\cdot\mathbf{a}_2 = -k_x/2 + \frac{\sqrt{3}k_y}{2}$, which maintains the original Dirac points on the honeycomb lattice at $(k_x, k_y) = (\pm 4\pi/3, 0)$ where $g_+g_- = -1$ and $f = 0$. When $t' = 0$, the dispersion near the Dirac point is $\varepsilon(k) = \pm\sqrt{3}tk/2$. When $t' \neq 0$, the low energy physics is controlled by t' and the dispersion near the Dirac points becomes $\varepsilon(k) = \pm t'k/2$. Simple dimension counting shows that the Hubbard term is perturbatively irrelevant in the weak coupling limit.

III. MAGNETIC INSTABILITIES AND AF ORDER

In this section we determine the magnetic phase boundaries by calculating the static spin susceptibility $\chi(\mathbf{q})$ by RPA. This kind of calculation is standard[44] so we only present the main results here and the details can be found in Appendix B.

We find that when $t'/t < 0.57$, the peak in $\chi(\mathbf{q})$ is located at the Γ point which means the magnetic phase is dominated by Néel order. For $t'/t > 0.57$, the peak splits into two, indicative of the tendency toward incommensurate AF order. Fig.2 (a) shows an example of the double-peak structure around the Γ in the susceptibility in the incommensurate Néel (i-Néel) regime. The magnetic phase diagram is shown in Fig.2 (b) where the SM and the magnetic phase boundary marks the onset of the divergence in the magnetic susceptibility $\chi(\mathbf{q})$[45]. The appearance of the i-Néel AF regime has the same origin as that of the Kitaev SL phase due to the competition between the Néel order and the rotated Néel order[39]. Microscopically, this competition arises from the t- and t'-terms and pushes the magnetic phase boundary dramatically toward large U, enabling the possible stable SL phases in the enlarged nonmagnetic regime in Fig.2 when $t'/t > 0.57$. In the following, we will focus on the $t'/t > 0.57$ regime and use the $SU(2)$ slave rotor theory to study the emergent SL phases.
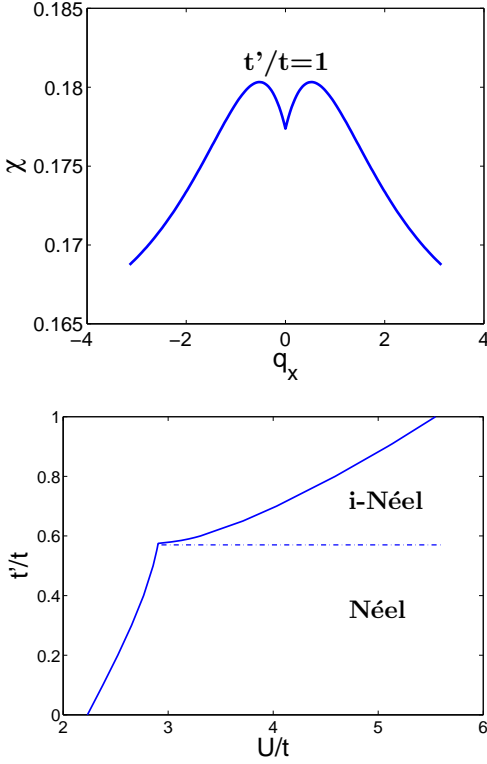
FIG. 2: (color online) Upper: An example of the double peaks of $\chi(\mathbf{q})$ in i-Néel regime. Lower: i-Néel refers to incommensurate AF order and there is no magnetic order in the blank area.

IV. $SU(2)$ SLAVE ROTOR THEORY

A. A brief review of $SU(2)$ slave rotor theory

Here we give a brief review of the $SU(2)$ slave rotor theory; more details can be found in[41,42]. We start from Eq.3 and decouple the Hubbard interaction by a Hubbard-Stratonovich (HS) transformation

$$\frac{i}{4}\sum_{i\in A,B}\mathrm{Tr}(\Psi_i\phi_i^a\sigma^a\Psi_i^\dagger)+\frac{3}{16U}\sum_{i\in A,B}\mathrm{Tr}(\phi_i^a\sigma^a)^2$$

where ϕ^a is a three-component HS field. To reveal the $SU(2)$ structure of the theory, we rotate the order parameters in the pseudo-spin space:

$$\phi_i^a\sigma^a\rightarrow Z_i^\dagger\phi_i^a\sigma^a Z_i$$

where Z_i is a time-dependent $SU(2)$ matrix and can be parametrized as:

$$Z_i=\begin{bmatrix} z_{i,1} & z_{i,2} \\ -z_{i,2}^* & z_{i,1}^* \end{bmatrix}$$

under the constraint $|z_{i,1}|^2+|z_{i,2}|^2=1$. Such a rotation transforms the electron operator Ψ_i to $F_i=\Psi_i Z_i^\dagger$ but

doesn't affect the spin operator $\mathbf{S}$. We thus call F_i the spinon carrying the spin degrees of freedom and Z_i the $SU(2)$ rotor tracking the pseudo-spin(charge) degrees of freedom. With a change of variable

$$\phi_i^a\sigma^a\rightarrow\phi_i^a\sigma^a+2iZ_i\partial_\tau Z_i^\dagger$$

the $SU(2)$ action reads

$$\begin{aligned} S = & S_t+\int_0^\beta d\tau\left\{\frac{1}{2}\sum_{i\in A,B}\mathrm{Tr}(F_i(\partial_\tau+\frac{i}{2}\phi_i^a\sigma^a)F_i^\dagger)\right. \\ & +\frac{1}{2U'}\sum_i\mathrm{Tr}(\frac{1}{2}\phi_i^a\sigma^a+iZ_i\partial_\tau Z_i^\dagger)^2 \\ & \left.+\sum_i i\lambda_i[\frac{1}{2}\mathrm{Tr}(Z_i^\dagger Z_i)-1]\right\}, \end{aligned} \tag{5}$$

with

$$\begin{aligned} S_t = & \int_0^\beta d\tau\left\{-t\sum_{\langle A,B\rangle}\mathrm{Tr}(Z_B Z_A^\dagger F_A^\dagger F_B)\right. \\ & \left.-t'\sum_{\langle A,B\rangle_a}\mathrm{Tr}(Z_B\sigma^z Z_A^\dagger F_A^\dagger\sigma^a F_B)\right\} \end{aligned} \tag{6}$$

where $U'=2U/3$ and λ_i is a local Lagrange multiplier imposing the $Z\in SU(2)$ constraint[46].

Eq.(5) describes a strongly coupled $SU(2)$ gauge theory, where Z and F are matter fields and ϕ are the temporal components of gauge fields. The gauge transformations are:

$$F_i\rightarrow F_iW_i,\ Z_i\rightarrow W_i^\dagger Z_i,\ \phi_i^a\sigma^a\rightarrow\phi_i^a\sigma^a-2iW_i\partial_\tau W_i^\dagger$$

The quartic matter fields in the hopping terms in Eq.(6) can be further decoupled using the HS transformation, giving the spatial components of gauge fields. Following Lee and Lee[47] we decouple the hopping terms:

$$\begin{aligned} S_t = & \int_0^\beta d\tau\left\{t\sum_{\langle A,B\rangle}\mathrm{Tr}(\eta_{AB}\eta_{AB}^\dagger)-t\sum_{\langle A,B\rangle}\mathrm{Tr}(\eta_{AB}Z_B Z_A^\dagger)\right. \\ & -t\sum_{\langle A,B\rangle}\mathrm{Tr}(\eta_{AB}^\dagger F_A^\dagger F_B)+t'\sum_{\langle A,B\rangle_a}\mathrm{Tr}(\eta'_{AB}\eta_{AB}'^\dagger) \\ & \left.-t'\sum_{\langle A,B\rangle_a}[\mathrm{Tr}(\eta'_{AB}Z_B\sigma^z Z_A^\dagger)+\mathrm{Tr}(\eta_{AB}'^\dagger F_A^\dagger\sigma^a F_B)]\right\} \end{aligned} \tag{7}$$

We can write[42] $\eta_{AB}=|\eta|e^{i\theta_{AB}}e^{i(c_{AB}^a-id_{AB}^a)\sigma^a}$ and $\eta'_{AB}=i|\eta'|e^{i\theta'_{AB}}e^{i(c_{AB}^{'a}-id_{AB}^{'a})\sigma^a}$. The action becomes complex for fluctuations of θ_{AB}, d_{AB}, ϕ_i and λ_i. To get saddle point solutions with real free energy we perform analytic continuations, $\theta_{AB}\rightarrow i\tilde\theta_{AB}$, $d_{AB}\rightarrow i\tilde d_{AB}$, $i\phi_i\rightarrow\tilde\phi_i$ and $i\lambda_i\rightarrow\tilde\lambda_i$, where quantities with tildes are real. We can obtain $\eta_{AB}=|\eta_Z|e^{i(c_{AB}^a+\check d_{AB}^a)\sigma^a}$, $\eta_{AB}^\dagger=|\eta_F|e^{-i(c_{AB}^a-\check d_{AB}^a)\sigma^a}$, $\eta'_{AB}=i|\eta'_Z|e^{i(c_{AB}'^a+\check d_{AB}'^a)\sigma^a}$ and

$\eta_{AB}^{'\dagger} = -i|\eta_F'|e^{-i(c_{AB}^{'a} - \tilde{d}_{AB}^{'a})\sigma^a}$. η/η' is a real/imaginary number times an $SU(2)$ matrix.

Since we are interested in the half filling case, we will take $\tilde{\phi}_i^a = 0$ ansätz for the temporal components of the gauge fields and relax the constraint by setting $\lambda_i = \lambda$, as is always done in slave particle theories. Despite the large gauge fluctuations, it is possible to obtain deconfined phases by different mean field ansätz[48].

B. Z_2 and $SU(2)$ SL phases

The generic ansätz,

$$\eta_{AB}^\dagger = a_F\sigma^0, \eta_{AB,a}^{'\dagger} = a_F'\sigma^a, \eta_{AB} = a_Z\sigma^0, \eta_{AB,a}' = a_Z'\sigma^a,$$

breaks the $SU(2)$ gauge symmetry to Z_2, where the subscript $a = x, y, z$ denotes the bond type. It preserves TRS and is not thus valid in the weak coupling. Denoting $t_\uparrow = -ta_F f - t'a_F'$, $t_\downarrow = -ta_F f + t'a_F'$, $\Delta_\uparrow = -t'a_F'(e^{ik_1} + e^{ik_2})$, and $\Delta_\downarrow = -t'a_F'(e^{ik_1} - e^{ik_2})$, the dispersion of the spinon is given by

$$\varepsilon_F = \pm\frac{1}{2}|t_\sigma \pm \Delta_\sigma|, \qquad (8)$$

which is the same as that obtained in[49,50]. The spinon band structure in the Z_2 phase is depicted in Fig. 3 (Upper panel). mean field equations are derived in Appendix C. There are two critical lines in the mean field solutions. For $U < U_{c1}$, the solution gives an improper p-wave superfluid phase that does not recover the SM when $U \to 0$. When $U > U_{c1}$, rotors are gapped and the Z_2 SL arises. Remarkably, a second critical line U_{c2} exists for $t'/t \lesssim 0.91$, such that when $U > U_{c2}$, a_F' and a_Z' vanish, i.e., the spin dependent hopping renormalizes to zero. The $SU(2)$ gauge symmetry is thus restored and the system enters an $SU(2)$ SL phase.

It is instructive to study the Z_2 ansätz for large-U more carefully and compare to exact results at $t'/t = 1$. The effective chemical potential of rotors is now $\lambda = U' = 2U/3$ and the Z_2 mean field equations are given by

$$a_Z = \frac{1}{6tN}\sum_{\mathbf{k}}\frac{\partial\varepsilon_{F,\sigma\pm}}{\partial a_F}, \quad a_Z' = \frac{1}{6t'N}\sum_{\mathbf{k}}\frac{\partial\varepsilon_{F,\sigma\pm}}{\partial a_F'} \qquad (9)$$

$$a_F = \frac{1}{24U'tN}\sum_{\mathbf{k}}\frac{\partial\varepsilon_{Z,\pm}^2}{\partial a_Z}, \quad a_F' = \frac{1}{24U't'N}\sum_{\mathbf{k}}\frac{\partial\varepsilon_{Z,\pm}^2}{\partial a_Z'},$$

where $\varepsilon_{F\sigma\pm}$ and $\varepsilon_{Z,\pm}$ are the spinon and the rotor dispersions respectively. $\varepsilon_{F\sigma\pm}$ gives Majorana fermion excitations at the Dirac point and six gapped flat bands. Note that $\varepsilon_{Z,\pm} \sim t$ and then $a_F, a_F' \sim t/U$, as expected for the charge and spin excitations in this limit. When $t = t'$, the velocity of the linear spinon dispersion in the Kitaev model, i.e., in the large U limit, is determined by $J = \frac{8t^2}{U}$. In order to be consistent with this velocity, the parameter a_F in the mean field spinon dispersion needs
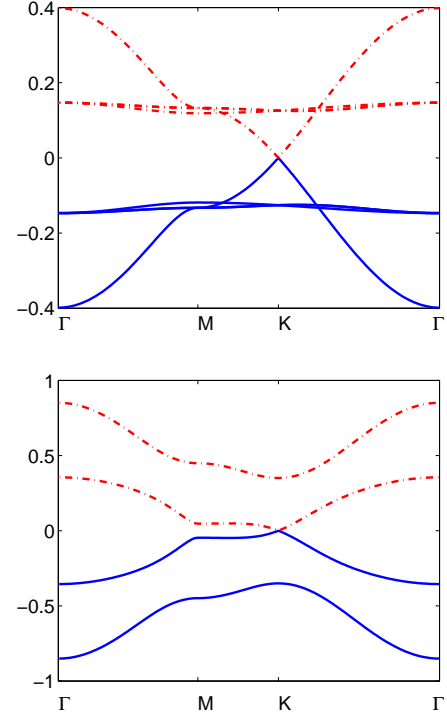

FIG. 3: (color online) Upper: Spinon band structure in Z_2 SL phase. $U = 4t$ and $t' = t$. Lower: Spinon band structure in $U(1)$ SL phase. $U = 3.67t$ and $t' = 0.9t$. Bands shown in blue solid line are occupied, in red dash line are unoccupied. Spinon dispersion in $SU(2)$ phase looks like the one in Z_2 phase with no (nearly) flat band.

to be rescaled to $a_F = \frac{J}{16t}$, which amounts to rescale the Hubbard U by a factor $\alpha \approx 0.572$ at $t'/t = 1$ (see Appendix C). Note that it is well-known that the Hubbard U needs to be rescaled in the mean field approximation of the slave rotor theory[46]. We would like to point out that the rescale of U only affects the results quantitatively. We will demonstrate below that α is essentially independent of t'/t in the regime where the slave rotor theory can be considered reliable. We solve the mean field equations self-consistently with the rescaled U.

C. $U(1)$ SL phases

To recover the semi-metal phase in small U regime, we consider the following ansätz,

$$\eta_{AB}^\dagger = a_F^0\sigma^0, \eta_{AB,a}^{'\dagger} = a_F^z\sigma^z, \eta_{AB} = a_Z^0\sigma^0, \eta_{AB,a}' = a_Z^z\sigma^z,$$

which breaks the $SU(2)$ gauge symmetry to $U(1)$ in general. The dispersion of the spinon is thus given by

$$\begin{aligned}
\varepsilon_F^2 &= t^2a_F^{02}|f|^2 + 3t'^2a_F^{z2} \pm \big[(t^2a_F^{02}|f|^2 + 3t'^2a_F^{z2})^2 \\
&\quad - |t'^2a_F^{z2}(g_+g_- + 1) - t^2a_F^{02}f^2|^2\big]^{1/2},
\end{aligned} \qquad (10)$$

which has the same form as Eq. (4) with renormalized hoppings $t \to ta_F^0$ and $t' \to t'a_F^z$. The spinon band structure in the $U(1)$ phase is depicted in Fig. 3 (Lower panel). Hence Hence, we expect it to be favored near the weak coupling where the TRS is broken. At the Dirac points, the linear dispersion $\varepsilon_F = \pm t'|a_F^z|k/2$. We again obtain two critical lines $\tilde{U}_{c1}$ and $\tilde{U}_{c2} > \tilde{U}_{c1}$. When $U < \tilde{U}_{c1}$, the rotors condense and the system is in the weak coupling SM phase. For $U > \tilde{U}_{c1}$, the rotors are gapped and the $U(1)$ SL phase emerges. For $U > \tilde{U}_{c2}$, both a_F^z and a_Z^z vanish and the system enters the $SU(2)$ SL phase.
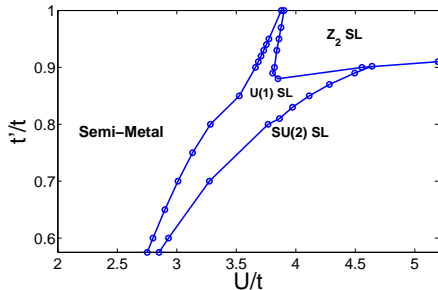

FIG. 4: (color online) Phase diagram of the SL states in the absence of magnetic order. Here we take $\alpha = 0.572$.

At a given point in the U/t - t'/t plane, which SL state is favored can be determined by comparing the mean field ground state energies among the $U(1)$, Z_2 and $SU(2)$ ansätz. The obtained slave-rotor phase diagram is shown in Fig.4.

Before ending this section, we discuss the stability of the SL states. To determine whether the SLs are stable one have to go beyond the mean field theory and consider the gauge fluctuations. We briefly discuss this issue here. The Z_2 spin liquid is stable because the gauge fluctuations are gapped. The $SU(2)$ spin liquid is the one study by Hermele[42], in this phase the low energy effective theory is gapless Dirac fermion coupled to compact $SU(2)$ gauge fields. Large N expansion shows that when the number of fermion flavors is large enough, this spin liquid phase is stable[42]. The effective theory of $U(1)$ spin liquid is gapless Dirac fermions coupled to compact $U(1)$ gauge field, this phase may also be stable against instanton effect[42,51,52].

V. DETERMINATION OF THE GLOBAL PHASE DIAGRAM

For the Kitaev-Hubbard model, in particular, a numerical calculation based on a variational cluster approximation and cluster perturbation theory showed that the SL phase is unstable against the SM and AF states when t'/t is smaller than a certain value[36]. We now explain how to combine the SL phase diagram in Fig.4 and the magnetic phase diagram in Fig. 2 to arrive at the global phase diagram shown in Fig.5. First, it is known when $t'/t \sim 1$ the slave rotor theory is reliable, while the RPA theory provides the leading magnetic instability for all t'/t. The numerical work in Ref.[36] showed that there is a tricritical point for the SL, SM and AF phases. This tricritical point in our result corresponds to the discontinuity point in the slope of the phase boundary in Fig. 2(b). Remarkably, we find that the lower bound of the SL phase touches the singular point of the magnetic phase boundary, forming the tricritical point observed by numerical simulations[36]. We stress that the tricritical point emerges in our theory without the need to change the rescaling factor α determined by the exact solution of the Kitaev model at $t'/t = 1$ and lends further support for an essentially t'/t-independent α in the SL regime. We emphasize that the topology of the SL phase diagram is not affected by varying α (see Appendix C 3). However, the tricritical point exists only if $\alpha \approx 0.572$. With increasing U, the $SU(2)$ SL becomes unstable to the AF i-Néel phase. However, the AF phase terminates when it meets the Z_2 SL because the Kitaev SL has lower energy. Finally, we would like to remark that although the general phase structure of our theory captures that of the numerical results with unprecedented symmetry distinct SL phases, the phase boundaries between the SM, AF and SL phases as well as the tricritical point only qualitatively agree with the numerical results in Refs.[21,22,36]. The exact determination of the phase boundaries is beyond the scope of the current work.

It's time to describe our main results shown in the phase diagram shown in Fig.5. Generally speaking, we found three types of phases: The SM phase for weak coupling, the AF phase for strong coupling $t'/t < 0.91$, and several SL states in-between. There are crucial differences between these new findings and the previous analytical and numerical results[32,36,39]. (i) The presence of three types of symmetry distinct gapless $U(1)$, $SU(2)$, and Z_2 SL phases that are experimentally distinguishable. While the Z_2 SL encloses the exact solvable Kitaev spin model[17] at $t'/t = 1$ and $t/U \ll 1$ and preserves the time-reversal symmetry (TRS), we discovered a TRS-breaking $U(1)$ SL that separates the Z_2 SL from the SM for $t'/t > 0.91$. The spinon dispersion in the $U(1)$ SL has the same form as that of the quasiparticle in the SM phase but with renormalized hoppings. For $t'/t < 0.91$, the $U(1)$ SL transforms with increasing U into the $SU(2)$ SL where a free Dirac fermion spinon dispersion arises with t' renormalized to zero and the TRS restored. (ii) Our RPA results captures qualitatively several different AF ordered phases in different parameter regions. The presence of the link-spin dependent hopping t' introduces a competition between conventional Néel order and a new type of AF order accompanied by a local spin rotation[39]. The latter pushes the magnetic phase boundary toward larger-U dramatically when $t'/t > 0.57$, realizing the various symmetry distinct SLs as stable phases of the electronic matter.
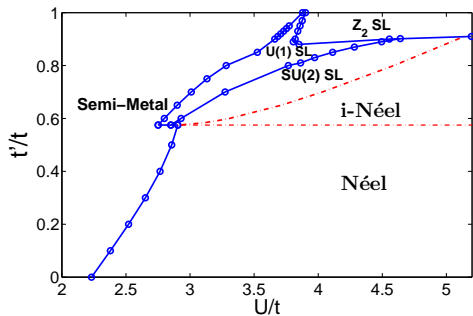
FIG. 5: (color online) Phase diagram. The magnetism part comes from Fig. 2(b) and the SL part from Fig. 4. We use the red dash-dot lines to separate the SL and AF phases as well as i-Neel and Neel because the RPA calculation in the strong coupling is not as good as that in the weak coupling.

VI. EXPERIMENTAL IMPLICATIONS

To sum up, we studied a Kitaev-Hubbard model using RPA and slave rotor theory. We obtained a fruitful phase diagram, including semi-metal phase, commensurate and incommensurate AFM ordered phases and three symmetry distinct SL states. We now discuss how to measure these phases in cold atom experiments.

If the SLs proposed are stable, they may be recognized in cold atom experiments. For example, Bragg spectroscopy can be used to measure the full band structure (see Fig.3) in cold atoms system[53]. There are some qualitative difference of the spinon dispersions in the Z_2, $U(1)$ and $SU(2)$ SL phases. The Z_2 SL differs apparently from the other two because there are Majorana fermion excitations and non-abelian anyonic Majorana bound states in an external magnetic field[17]. The $U(1)$ spinon is of a linear dispersion proportional to $t'|a_F^z|$ at the Dirac points and does not have a conserved S^z, the dispersion of the $SU(2)$ spinon is the same as that of the free Dirac fermion with a conserved S^z and a renormalized hopping ta_F^0.

Bragg spectroscopy can also be used to determine the dynamical spin structure $S^{+-}(\omega, \mathbf{q})$, which is the Fourier transformation of spin-spin correlation $\langle S^+(\mathbf{r}, t)S^-(\mathbf{r}', t')\rangle$ and proportional to the cross section of Bragg scattering[54] . In the $U(1)$ SL phase, because of the spin flip terms in the effective spinon Hamiltonian, $S^{+-}(\omega, \mathbf{q} = 0) \neq 0$. In the small ω limit the cross section is proportional to the density of states near the Fermi surface (Dirac points), so $S^{+-}(\omega, \mathbf{q} = 0) \propto \omega$ for small ω (see Fig.6 Upper panel). In the Z_2 spin liquid phase, $S^{+-}(\omega, \mathbf{q} = 0) = 0$ if ω is smaller than the gap of the (nearly) flat band and a sharp peak appears when the energy transfer is twice the gap (see Fig.6 Lower panel). In contrast, $S^{+-}(\omega, \mathbf{q} = 0) = 0$ in $SU(2)$ SL phase. These properties can be used to distinguish the SLs.

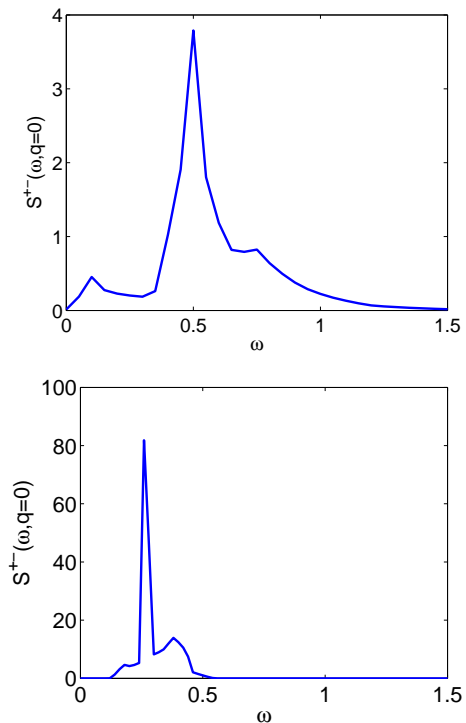The anti-ferromagnet order can also be measured via Bragg scattering[55].

FIG. 6: (color online) Upper: Dynamical spin structure factor in $U(1)$ spin liquid phase. $U = 3.67t$ and $t' = 0.9t$. Lower: Dynamical spin structure factor in Z_2 spin liquid phase. $U = 4t$ and $t' = t$

Appendix A: Symmetries of t'-term

If Ψ_A is redefined as

$$\Psi_A = \begin{bmatrix} c_{A\uparrow} & -c_{A\downarrow}^\dagger \\ c_{A\downarrow} & c_{A\uparrow}^\dagger \end{bmatrix}$$

then the t'-term can be written as

$$-t' \sum_{\langle A,B\rangle_a} \text{Tr}(\Psi_A^\dagger \sigma^a \Psi_B)$$

which is pseudo-spin rotational invariant.

To reveal the spin-rotational symmetry of t'-term, one can enlarge the unit cell and perform local spin rotations of Ψs (see Fig.7): for circle , $\Psi \to \Psi$, for square, $\Psi \to \sigma^z \Psi$, for diamond, $\Psi \to \sigma^y \Psi$, for triangle, $\Psi \to$

$\sigma^x \Psi$. After this rotation, t'-term can can be written in spin-rotational invariant way. However, even after this rotation, t'-term can't be written as the same form as t-term. Because for t'-term, electron acquire π phase when hopping around a hexagon and this phase can not be removed by spin rotations.

Note that the symmetry operations of t-term and t'-term are not compatible, that's to say, t-term is invariant under some operations while t'-term is invariant under others, so both symmetries are broken when t and t' are nonzero.
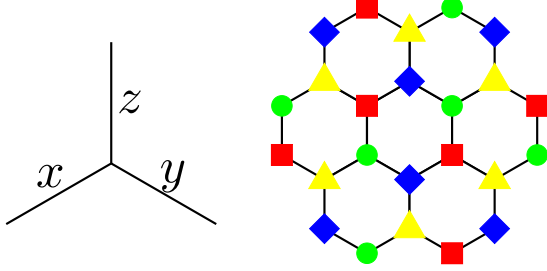

FIG. 7: (color online) t'-term can be written in a spin rotational invariant manner if the unit cell is enlarged.

Appendix B: Calculation of spin susceptibility

The partition function is $Z = \int Df^\dagger Df e^{-\int_0^\beta L d\tau}$, where

$$L = \sum f_{i\sigma}^\dagger (\partial_\tau \delta_{ij}\delta_{\sigma\sigma'} - t_{ij}^{\sigma\sigma'})f_{j\sigma'} + U\sum n_{i\uparrow}n_{i\downarrow}$$

After performing a Hubbard-Stratonovich transformation in spin channel, we get: $Z = \int Df^\dagger Df D\phi e^{-S}$ and

$$S = \int_0^\beta d\tau \sum_i f_i^\dagger \partial_\tau f_i - t \sum_{\langle ij \rangle_a} f_i^\dagger (I + \sigma^a) f_j + \frac{U}{4}\sum_i \phi_i^2 + \frac{U}{2}\sum_i \phi_i f_i^\dagger \sigma^z f_i$$

Integrating out fermions we get the effective action

$$S_{\text{eff}} = \frac{U}{4}\int_0^\beta d\tau \sum \phi_i(\tau)^2 - \text{Trln}[\partial_\tau - t_{i,j}^{\sigma\sigma'} + \frac{U}{2}\sigma\phi_i]$$

Setting $\phi_A = -\phi_B = \phi$, then up to second order and in

static limit: $S_{\text{eff}} = \sum_{\mathbf{q}} \frac{U}{4}[1 - U\chi(\mathbf{q})]\phi(\mathbf{q})\phi(-\mathbf{q})$ where $\chi(\mathbf{q}) = -\frac{1}{2\beta N}\sum_{\mathbf{k},\omega_n} \text{Tr} G_0(i\omega_n, \mathbf{k})\sigma^z \otimes \tau^z G_0(i\omega_n, \mathbf{k} + \mathbf{q})\sigma^z \otimes \tau^z$ and $G_0(i\omega_n, \mathbf{k}) = \frac{1}{i\omega_n - \mathcal{H}(\mathbf{k})}$ is bare Green's function. If $\mathcal{H}$ is diagonalized by a matrix V, i.e., $V^\dagger(\mathbf{k})\mathcal{H}(\mathbf{k})V(\mathbf{k}) = diag(E_{h\mathbf{k}}, -E_{h\mathbf{k}}, E_{l\mathbf{k}}, -E_{l\mathbf{k}})$, then

$$\chi(\mathbf{q}) = \frac{1}{2N}\sum_{\mathbf{k}} \frac{W_{12\mathbf{k},\mathbf{q}}W_{21\mathbf{k},-\mathbf{q}}}{E_{h\mathbf{k}-\mathbf{q}/\mathbf{2}} + E_{h\mathbf{k}+\mathbf{q}/\mathbf{2}}} + \frac{W_{14\mathbf{k},\mathbf{q}}W_{41\mathbf{k},-\mathbf{q}}}{E_{h\mathbf{k}-\mathbf{q}/\mathbf{2}} + E_{l\mathbf{k}+\mathbf{q}/\mathbf{2}}} + \frac{W_{21\mathbf{k},\mathbf{q}}W_{12\mathbf{k},-\mathbf{q}}}{E_{h\mathbf{k}+\mathbf{q}/\mathbf{2}} + E_{h\mathbf{k}-\mathbf{q}/\mathbf{2}}} + \frac{W_{23\mathbf{k},\mathbf{q}}W_{32\mathbf{k},-\mathbf{q}}}{E_{l\mathbf{k}+\mathbf{q}/\mathbf{q}} + E_{h\mathbf{k}-\mathbf{q}/\mathbf{2}}}$$

$$+ \frac{1}{2N}\sum_{\mathbf{k}} \frac{W_{32\mathbf{k},\mathbf{q}}W_{23\mathbf{k},-\mathbf{q}}}{E_{l\mathbf{k}-\mathbf{q}/\mathbf{2}} + E_{h\mathbf{k}+\mathbf{q}/\mathbf{2}}} + \frac{W_{34\mathbf{k},\mathbf{q}}W_{43\mathbf{k},-\mathbf{q}}}{E_{l\mathbf{k}-\mathbf{q}/\mathbf{2}} + E_{l\mathbf{k}+\mathbf{q}/\mathbf{2}}} + \frac{W_{41\mathbf{k},\mathbf{q}}W_{14\mathbf{k},-\mathbf{q}}}{E_{l\mathbf{k}-\mathbf{q}/\mathbf{2}} + E_{h\mathbf{k}+\mathbf{q}/\mathbf{2}}} + \frac{W_{43\mathbf{k},\mathbf{q}}W_{34\mathbf{k},-\mathbf{q}}}{E_{l\mathbf{k}+\mathbf{q}/\mathbf{2}} + E_{l\mathbf{k}-\mathbf{q}/\mathbf{2}}} \quad \text{(B1)}$$

where $W(\mathbf{k}, \mathbf{q}) = V^\dagger(\mathbf{k} - \mathbf{q}/2)\sigma^z \otimes \tau^z V(\mathbf{k} + \mathbf{q}/2)$. $W(\mathbf{k}, \mathbf{q}) = W^\dagger(\mathbf{k}, -\mathbf{q})$. Because of the inversion symmetry, we have $V(-\mathbf{k}) = \sigma^x \otimes \tau^0 V(\mathbf{k})$, then $W(\mathbf{k}, \mathbf{q}) = -W(-\mathbf{k}, -\mathbf{q})$. Using this relation, Eq.(B1) can be simplified:

$$\chi(\mathbf{q}) = \frac{1}{N}\sum_{\mathbf{k}} \left[\frac{W_{12\mathbf{k},\mathbf{q}}W_{21\mathbf{k},-\mathbf{q}}}{E_{h\mathbf{k}-\mathbf{q}/\mathbf{2}} + E_{h\mathbf{k}+\mathbf{q}/\mathbf{2}}} \right.$$

$$\left. + \frac{2W_{14\mathbf{k},\mathbf{q}}W_{41\mathbf{k},-\mathbf{q}}}{E_{h\mathbf{k}-\mathbf{q}/\mathbf{2}} + E_{l\mathbf{k}+\mathbf{q}/\mathbf{2}}} + \frac{W_{34\mathbf{k},-\mathbf{q}}W_{43\mathbf{k},\mathbf{q}}}{E_{l\mathbf{k}-\mathbf{q}/\mathbf{2}} + E_{l\mathbf{k}+\mathbf{q}/\mathbf{2}}} \right]$$

Note that both anti-ferromagnetic order and ferromagnetic order preserve translational symmetry on honeycomb lattice. Peak at Γ point indicts anti-ferromagnetic order because we have set $\phi_A = -\phi_B = \phi$.

Appendix C: Mean field theory of $SU(2)$ slave rotor theory

1. Z_2 ansätz

The ansätz $\eta_{AB}^\dagger = a_F\sigma^0, \eta_{AB,a}^{'\dagger} = a_F'\sigma^a, \eta_{AB} = a_Z\sigma^0, \eta_{AB,a}' = a_Z'\sigma^a$ breaks the $SU(2)$ gauge symmetry to Z_2. As this ansätz preserves time reversal symmetry, it works for large U. In this case, the effective Lagrangian reads:

$$\mathcal{L} = \sum_{i\in A,B}(f_{i\sigma}^\dagger\partial_\tau f_{i\sigma}) + \frac{3}{2U\alpha}\sum_{i\in A,B}(\partial_\tau z_\alpha^*\partial_\tau z_\alpha)$$
$$-\lambda\sum_{i\in A,B}(z_\alpha^*z_\alpha-1) + 6tNa_F^0a_Z^0 + 6t'Na_F^{'}a_Z^{'}$$
$$-t\sum_{\langle A,B\rangle}a_F f_{A\sigma}^\dagger f_{B\sigma} - t'\sum_{\langle A,B\rangle_x}a_F'\sigma f_{A\sigma}^\dagger f_{B\sigma}^\dagger$$
$$-t'\sum_{\langle A,B\rangle_y}a_F' f_{A\sigma}^\dagger f_{B\sigma}^\dagger - t'\sum_{\langle A,B\rangle_z}a_F'\sigma f_{A\sigma}^\dagger f_{B\sigma}$$
$$-t\sum_{\langle A,B\rangle}a_Z z_{A\alpha}^\dagger z_{B\alpha} + t'\sum_{\langle A,B\rangle_x}a_Z' z_{A\alpha}^\dagger z_{B\beta}^\dagger$$
$$-t'\sum_{\langle A,B\rangle_y}ia_Z' z_{A\alpha}^\dagger z_{B\beta}^\dagger - t'\sum_{\langle A,B\rangle_z}a_Z'\alpha z_{A\alpha}^\dagger z_{B\alpha}$$

Let $t_\uparrow = -ta_F f - t'a_F'$, $t_\downarrow = -ta_F f + t'a_F'$, $\Delta_\uparrow = -t'a_F'(e^{ik_1}+e^{ik_2})$ and $\Delta_\downarrow = -t'a_F'(e^{ik_1}-e^{ik_2})$, then eigenvalues of spinons are $\varepsilon_F = \pm\frac{1}{2}|t_\sigma\pm\Delta_\sigma|$, of rotors are $(\varepsilon_Z-\lambda)^2 = t^2a_Z^2 ff^* + 3t'^2a_Z'^2 \pm \sqrt{(t^2a_Z^2 ff^*+3t'^2a_Z'^2)^2 - |t'^2a_Z'^2(g_+g_-+1) - t^2a_Z^2 f^2|^2}$. If $a_Z't' < 2.8ta_Z$, the minimal of rotor eigenvalues is at Γ point. In the following we assume $a_Z't' < 2.8ta_Z$ and we find this condition is satisfied. The rotor condensed part is: $-3ta_Z N(z_{A1}^*z_{B1} + z_{A2}^*z_{B2}) + t'a_Z'(1+i)(z_{A1}z_{B2}+z_{A2}z_{B1}) - t'a_Z'(z_{A1}^*z_{B1} - z_{A2}^*z_{B2}) + \lambda N z_{A/B\alpha}^* z_{A/B\alpha}/2 + h.c.$ and $\lambda_{min} = 3ta_Z + \sqrt{3}t'a_Z'$. Let $\sum_{i\in A,B}z_{i\alpha}^*z_{i\alpha} = 2z^2$, then $z_{A2}=z_{B2}=2z/\sqrt{6+2\sqrt{3}}$, $z_{B1}=z_{A1}=(i-1)(1+\sqrt{3})z/\sqrt{6+2\sqrt{3}}$, so the rotor condensed part becomes: $-6ta_Z Nz^2 - 2\sqrt{3}t'a_Z'Nz^2 + 2\lambda Nz^2$. The free energy is($U' = 2\alpha U/3$):

$$F = -T\sum_{\mathbf{k},i}\ln(1+e^{-\beta\varepsilon_{F,i}})$$
$$+T\sum_{\omega_n}\sum_{\mathbf{k},i}\ln(\frac{3\omega_n^2}{2U}+\varepsilon_{Z,i}) + \text{const}$$
$$= -T\sum_{\mathbf{k},i}\ln(1+e^{-\beta\varepsilon_{F,i}}) + \sum_{\mathbf{k},i}\sqrt{U'\varepsilon_{Z,i}}$$
$$+2T\sum_{\mathbf{k},i}\ln(1-e^{-\beta\sqrt{U'\varepsilon_{Z,i}}}) + \text{const} \quad (C1)$$

where the constant term is $-2N\lambda + 6tNa_Fa_Z + 6t'Na_F'a_Z' - 6ta_Z Nz^2 - 2\sqrt{3}t'a_Z'Nz^2 + 2\lambda Nz^2$ and the

second term in the last line is zero point energies of relativistic rotors. Taking derivatives with respect to the parameters we get the following self-consistent equations:

$$\frac{\partial F}{\partial a_F} = \sum_{\mathbf{k},i}n_f(\varepsilon_{F,i})\frac{\partial\varepsilon_{F,i}}{\partial a_F} + 6tNa_Z = 0$$
$$\frac{\partial F}{\partial a_F^z} = \sum_{\mathbf{k},i}n_f(\varepsilon_{F,i})\frac{\partial\varepsilon_{F,i}}{\partial a_F'} + 6t'Na_Z' = 0$$
$$\frac{\partial F}{\partial a_Z} = \sum_{\mathbf{k},i}\frac{\sqrt{U'}}{2\sqrt{\varepsilon_{Z,i}}}\coth(\frac{\beta\sqrt{U'\varepsilon_{Z,i}}}{2})\frac{\partial\varepsilon_{Z,i}}{\partial a_Z}$$
$$+6tN(a_F-z^2) = 0 \quad (C2)$$
$$\frac{\partial F}{\partial a_Z'} = \sum_{\mathbf{k},i}\frac{\sqrt{U'}}{2\sqrt{\varepsilon_{Z,i}}}\coth(\frac{\beta\sqrt{U'\varepsilon_{Z,i}}}{2})\frac{\partial\varepsilon_{Z,i}}{\partial a_Z'}$$
$$+6t'N(a_F'-z^2/\sqrt{3}) = 0$$
$$\frac{\partial F}{\partial\lambda} = \sum_{\mathbf{k},i}\frac{\sqrt{U'}}{2\sqrt{\varepsilon_{Z,i}}}\coth(\frac{\beta\sqrt{U'\varepsilon_{Z,i}}}{2}) - 2N + 2Nz^2 = 0$$

Solving them numerically, we also find two critical lines. When the interaction is smaller than U_{c1} we predict a $p-wave$ super-conducting phase which is not reliable. When $U > U_{c1}$ we get spin liquid phase, in both cases the spinons are gapless.

In the spin liquid regime, when $t'/t \lesssim 0.91$ and $U > U_{c2}$, we get an $SU(2)$ spin liquid with $a_F' = a_Z' = 0$. Otherwise it's a Z_2 spin liquid (See, e.g., Fig.8(a)).

We study the large U limit of Z_2 ansätz at $t' = t = 1$ carefully. From Eq.(C2), we know that in the large U limit the effective chemical potential of rotors is $\lambda = U'$. Writing $\varepsilon_{F\sigma\pm} = \frac{1}{2}|t_\sigma\pm\Delta_\sigma|$, and $\varepsilon_\pm = [t^2a_Z^2 ff^*+3t'^2a_Z'^2\pm((t^2a_Z^2 ff^*+3t'^2a_Z'^2)^2 - |t'^2a_Z'^2(g_+g_-+1) - t^2a_Z^2 f^2|^2)^{1/2}]^{1/2}$, then in the large U limit Eq.(C2) becomes:

$$a_Z = \frac{1}{6tN}\sum_{\mathbf{k}}\frac{\partial\varepsilon_{F,\sigma\pm}}{\partial a_F}, \quad a_Z' = \frac{1}{6t'N}\sum_{\mathbf{k}}\frac{\partial\varepsilon_{F,\sigma\pm}}{\partial a_F'} \quad (C3)$$
$$a_F = \frac{1}{24U'tN}\sum_{\mathbf{k}}\frac{\partial\varepsilon_{Z,\pm}^2}{\partial a_Z}, \quad a_F' = \frac{1}{24U't'N}\sum_{\mathbf{k}}\frac{\partial\varepsilon_{Z,\pm}^2}{\partial a_Z'},$$

If $t' = t$ and U is large enough, $a_F' = a_F$(See, Fig.8(a)). Then the spinon dispersion becomes: $\varepsilon_{F\uparrow+} = ta_F|f|$ and $\varepsilon_{F\uparrow-} = \varepsilon_{F\downarrow\pm} = ta_F$. We find two gapless dispersing bands and six gapped flat bands, which matches the exact solution of Kitaev model. In order to be consistent with this velocity, the mean field parameter a_F in the mean field spinon dispersion needs to be rescaled to $a_F = \frac{J}{16t}$[17,49]. Solving Eq.C3 we find $a_FU' = 0.1906t$, which gives $\alpha = 0.572$. For $t' \neq t$, $a_F \neq a_F'$, the gapped flat bands acquire a weak dispersion[50].
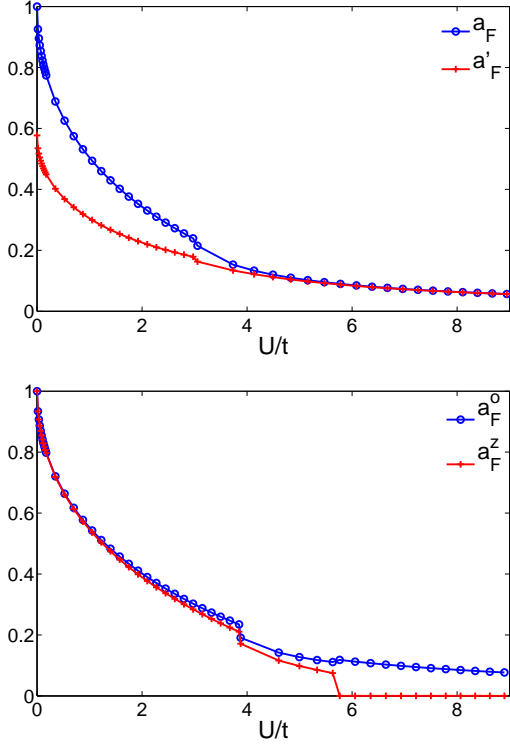
FIG. 8: (color online) Upper: a_F and a'_F for Z_2 ansätz. at $t = t' = 1$. $a'_F/a_F \to 1$ when U increases. Lower: a_F^0 and a_F^z for $U(1)$ ansätz at $t = t' = 1$. There are two phase transitions at $U_{c1} \approx 3.9t$ and $U_{c2} \approx 5.8t$.

2. $U(1)$ ansätz

The ansätz $\eta_{AB}^\dagger = a_F^0 \sigma^0, \eta_{AB,a}'^\dagger = a_F^z \sigma^z, \eta_{AB} = a_Z^0 \sigma^0, \eta_{AB,a}' = a_Z^z \sigma^z$ breaks the $SU(2)$ gauge symmetry to $U(1)$. The spinon Hamiltonian has the same form as the noninteracting electron Hamiltonian with normalized hopping in this ansätz. We expect it is applicable to a small U. The symmetry of this ansätz is the same as the original model, e.g., time reversal symmetry is broken. As time reversal symmetry restores in the large U limit, this ansätz does not work. The effective Lagrangian is:

$$
\begin{aligned}
\mathcal{L} = & \sum_{i \in A,B} f_{i\sigma}^\dagger \partial_\tau f_{i\sigma} + \frac{3}{2U\alpha} \sum_{i \in A,B} (\partial_\tau z_{i\alpha}^* \partial_\tau z_{i\alpha}) \\
& + \lambda \sum_{i \in A,B} (z_{i\alpha}^* z_{i\alpha} - 1) + 6tN a_F^0 a_Z^0 + 6t'N a_F^z a_Z^z \\
& - t a_F^0 \sum_{\langle A,B \rangle} f_{A\sigma}^\dagger f_{B\sigma} - t' a_F^z \sum_{\langle A,B \rangle_a} f_{A\sigma}^\dagger \sigma_{\sigma\sigma'}^a f_{B\sigma'} \\
& - t a_Z^0 \sum_{\langle A,B \rangle} z_{A\alpha}^\dagger z_{B\alpha} - t' a_Z^z \sum_{\langle A,B \rangle} z_{A\alpha}^\dagger \sigma_{\alpha\beta}^z z_{B\beta}
\end{aligned}
$$

Dispersion of spinons are $\varepsilon_F^2 = t^2 a_F^{02} f f^* + 3t'^2 a_F^{z2} \pm [(t^2 a_F^{02} f f^* + 3t'^2 a_F^{z2})^2 - |t'^2 a_F^{z2}(g_+ g_- + 1) - t^2 a_F^{02} f^2|^2]^{1/2}$. At Dirac points, the linear dispersion is proportional

to t' and is not degenerate if $SU(2)$ symmetry is not restored. When, $a_F^z = 0$, the $SU(2)$ gauge symmetry is restored, the dispersion becomes two-fold degenerate $\varepsilon = \pm t|a_F^0||f|$, which is the same as the free Dirac fermion on the honeycomb lattice with the renormalized hopping $t|a_F^0|$. The dispersion of rotors are $\varepsilon_Z = \lambda \pm |(ta_Z^0 \pm t'a_Z^z)f|$. Rotors may condense at Γ point, and we can write the condensed part explicitly($z_A = z_B$): $-6Nta_Z^0(z_1^2 + z_2^2) - 6Nt'a_Z^z(z_1^2 - z_2^2) + 2N\lambda(z_1^2 + z_2^2)$. The free energy is the same form as Eq.C1 with the constant term replaced by $-2N\lambda + 6tNa_F^0 a_Z^0 + 6t'N a_F^z a_Z^z - 6Nta_Z^0(z_1^2 + z_2^2) - 6Nt'a_Z^z(z_1^2 - z_2^2) + 2N\lambda(z_1^2 + z_2^2)$. Since $a_Z^0, a_Z^z > 0$, we have $z_2 = 0$ and $\lambda_{min} = 3(ta_Z^0 + t'a_Z^z)$. Taking derivatives with respect to the parameters we get the following self-consistent equations:

$$
\begin{aligned}
\frac{\partial F}{\partial a_F^0} = & \sum_{\mathbf{k},i} n_f(\varepsilon_{F,i}) \frac{\partial \varepsilon_{F,i}}{\partial a_F^0} + 6tN a_Z^0 = 0 \\
\frac{\partial F}{\partial a_F^z} = & \sum_{\mathbf{k},i} n_f(\varepsilon_{F,i}) \frac{\partial \varepsilon_{F,i}}{\partial a_F^z} + 6t'N a_Z^z = 0 \\
\frac{\partial F}{\partial a_Z^0} = & \sum_{\mathbf{k},i} \frac{\sqrt{U'}}{2\sqrt{\varepsilon_{Z,i}}} \coth\left(\frac{\beta \sqrt{U' \varepsilon_{Z,i}}}{2}\right) \frac{\partial \varepsilon_{Z,i}}{\partial a_Z^0} \\
& + 6tN(a_F^0 - z_1^2) = 0 \qquad\qquad\text{(C4)} \\
\frac{\partial F}{\partial a_Z^z} = & \sum_{\mathbf{k},i} \frac{\sqrt{U'}}{2\sqrt{\varepsilon_{Z,i}}} \coth\left(\frac{\beta \sqrt{U' \varepsilon_{Z,i}}}{2}\right) \frac{\partial \varepsilon_{Z,i}}{\partial a_Z^z} \\
& + 6t'N(a_F^z - z_1^2) = 0 \\
\frac{\partial F}{\partial \lambda} = & \sum_{\mathbf{k},i} \frac{\sqrt{U'}}{2\sqrt{\varepsilon_{Z,i}}} \coth\left(\frac{\beta \sqrt{U' \varepsilon_{Z,i}}}{2}\right) - 2N + 2Nz_1^2 = 0
\end{aligned}
$$

Solving these self-consistent equations numerically we find two critical lines: when the interaction is smaller than $\tilde{U}_{c1}$ we get a semi-metal phase, otherwise the rotors are gapped and we get a spin liquid phase. We find that a_F^z and a_Z^z are strongly suppressed when increasing U and they vanish if $U > \tilde{U}_{c2}$. In this case we actually get an $SU(2)$ spin liquid, see Fig.8(b) . This can be understood in the following way: in the large U limit there is an emergent time reversal symmetry, and there are two ways to recover this symmetry, that's, $a_F^z = a_Z^z = 0$ or $a_F^0 = a_Z^0 = 0$, because we are considering the $t' < t$ case, we get $a_F^z = a_Z^z = 0$. This indicates that the $U(1)$ ansätz is not reliable in the large U limit.

3. α dependence of spin liquid phase diagram

In the main text we choose $\alpha = 0.572$ and get the spin liquid phase diagram Fig.4. We have explained why we choose the rescale parameter α as t'/t-independent. However, one may wonder[56] what the phase diagram looks like if α is dependent on t'/t. The answer is t'/t-dependence of α doesn't change the topology of the spin liquid phase digram because α is only a rescale of the

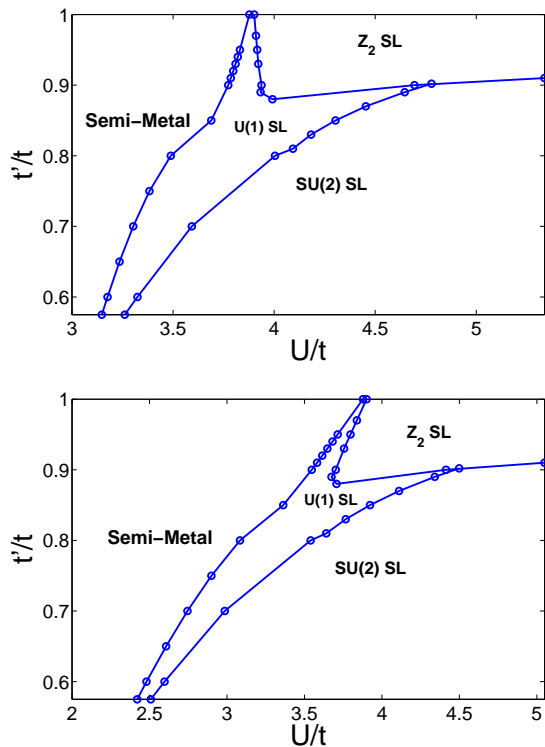interaction. To show this we plot the phase diagram for different dependence of α on t'/t (Fig.9).

FIG. 9: (color online) $\alpha(t'/t = 1) = 0.572$ and varies linearly with t'/t. Upper: $\alpha(t'/t = 0.575) = 0.5$. Lower: $\alpha(t'/t = 1) = 0.572$, $\alpha(t'/t = 0.575) = 0.65$.

[1] P. Fazekas and P. W. Anderson, Philos. Mag. **30**, 423 (1974).

[2] P. W. Anderson, Science **235**, 1196 (1987).

[3] P. A. Lee, Science **321**, 1306 (2008).

[4] Y. Shimizu, K. Miyagawa, K. Kanoda, M. Maesato, and G. Saito, Phys. Rev. Lett. **91**, 107001 (2003).

[5] J. S. Helton, K. Matan, M. P. Shores, E. A. Nytko, B. M. Bartlett, Y. Yoshida, Y. Takano, A. Suslov, Y. Qiu, J.-H. Chung, D. G. Nocera, and Y. S. Lee, Phys. Rev. Lett. **98**,107204(2007).

[6] Y. Okamoto, M. Nohara, H. Aruga-Katori, and H. Takagi, Phys. Rev. Lett. **99**, 137207(2007).

[7] T. Itou, A. Oyamada, S. Maegawa, M. Tamura, and R. Kato, Phys. Rev. B **77**, 104413 (2008).

[8] T.-H. Han, J. S. Helton, S. Chu, D. G. Nocera, J. A. Rodriguez-Rivera, C. Broholm and Y. S. Lee, Nature **492**, 406(2012).

[9] R. H. Colman, C. Ritter, and A. S. Wills, Chem. Mater. **20**, 6897 (2008).

[10] H. C. Jiang, Z. Y. Weng, and D. N. Sheng, Phys. Rev. Lett. **101**, 117203 (2008).

[11] S. Yan, D. A. Huse, and S. R. White, Science **332**, 1173(2011).

[12] H. C. Jiang, H. Yao and L. Balents, Phys. Rev. B **86**, 024424(2012).

[13] S. Depenbrock, I. P. McCulloch, and U. Schollwck, Phys. Rev. Lett. **109**, 067201(2012).

[14] H. C. Jiang, Z. H. Wang and L. Balents, Nature Physics

8,902(2012).

[15] P. Fendley, R. Moessner, and S. L. Sondhi, Phys. Rev. B **66**, 214513 (2002).

[16] A. Y. Kitaev, Annals. Phys., **303**, 2(2003).

[17] A. Y. Kitaev, Annals. Phys., **321**, 2(2006).

[18] M. Levin, and X. G. Wen, Phys. Rev. B **71**, 045110(2005).

[19] Hong Yao and Steven A. Kivelson, Phys. Rev. Lett. **99**, 247203(2007).

[20] Hong Yao and Dung-Hai Lee, Phys. Rev. Lett. **107**, 087205(2011).

[21] Z. Y. Meng, T. C. Lang, S. Wessel, F. Assand, and A. Muramatsu, Nature (London) **464**, 847 (2010).

[22] S. Sorella, Y. Otsuka, and S. Yunoki, Sci. Rep. **2**, 992 (2012).

[23] F. F. Assaad and I. F. Herbut, Phys. Rev. X **3**, 031010(2013).

[24] W. Wu, Y. -H. Chen, H.-S. Tao, N.-H. Tong, and W.-M. Liu, Phys. Rev. B **82**, 245102 (2010).

[25] A. Liebsch, Phys. Rev. B **83**, 035113 (2011).

[26] R.-Q. He and Z.-Y. Lu, Phys. Rev. B **86**, 045105 (2012).

[27] S. R. Hassan and D. Senechal, Phys. Rev. Lett. **110**, 096402 (2013).

[28] A. Liebsch, arXiv: 1302.6547 (2013).

[29] Y. Zhou and T. K. Ng, Phys. Rev. B **88**, 165130 (2013).

[30] S. Zhou, Y. P. Wang, and Z. Wang, Phys. Rev. B **89**, 195119 (2014)..

[31] G. -Y. Sun and S.-P. Kou, J. Phys: Condens. Matter **23**, 045603 (2011).

[32] L. M. Duan, E. Demler, and M. D. Lukin, Phys. Rev. Lett. **91**, 090402(2003).

[33] C. Zhang, V. W. Scarola, S. Tewari, S. Das Sarma, Proc. Natl. Acad. Sci. USA **104**, 18415 (2007).

[34] P. V. Sriluckshmy, A. Mishra, S. R. Hassan, and R. Shankar, Phys. Rev. B **89**, 045105(2014).

[35] S. R. Hassan, Sandeep Goyal, R. Shankar, and David Snchal, Phys. Rev. B **88**, 045301(2013).

[36] S. R. Hassan, P. V. Sriluckshmy, Sandeep K. Goyal, R. Shankar, and David Sénéchal, Phys. Rev. Lett. **110**, 037201(2013).

[37] J. P. L. Faye, D. Sénéchal and S. R. Hassan, Phys. Rev. B **89**, 115130(2014).

[38] For a recent review , see Z. Nussinov and J van den Brink, arXive 1303.5922.

[39] Y. Yu, L. Liang, Q. Niu and S. J. Qin, Phys. Rev. B **87**, 041107(RC) (2013).

[40] X. G. Wen, *Quantum Field Theory of Many-Body Systems* (Oxford University Press, 2004).

[41] K.-S. Kim, Phys. Rev. Lett. **97**, 136402 (2006); Phys. Rev. B **75**, 245105(2007).

[42] M. Hermele, Phys. Rev. B **76**, 035125(2007).

[43] I. Affleck, Z. Zou, T. Hsu, and P. W. Anderson, Phys. Rev. B **38**, 745(1988).

[44] See, for example, N. Nagaosa, *Quantum Field Theory in Strongly Correlated Electronic Systems*, (Springer, 1999).

[45] The different magnetic properties versus different hopping processes Similar phenomenon was also found in a corrected topological insulator model. See, M. Kargarian, A. Langari, and G. A. Fiete, Phys. Rev. B **86**, 205124 (2012).

[46] S. Florens and A. Georges, Phys. Rev. B**70**,035114(2004).

[47] S.-S. Lee and P. A. Lee, Phys. Rev. Lett. **95**, 036403(2005).

[48] P. A. Lee, N. Nagaosa and X.-G. Wen, Rev. Mod. Phys. **78**, 17(2006).

[49] F. J. Burnell and C. Nayak, Phys. Rev. B **84**, 125125(2011).

[50] R. Schaffer, S. Bhattacharjee and Y. B. Kim, Phys. Rev.B **86**, 224417(2012).

[51] M. Hermele, T. Senthil, M. P. A. Fisher, P. A. Lee, N. Nagaosa, and X.-G. Wen, Phys. Rev. B **70**, 214437 (2004).

[52] S.-S. Lee, Phys. Rev. B **78**, 085129 (2008).

[53] J. Heinze, S. Götze, J. S. Krauser, B. Hundt, N. Fläschner, D.-S. Lühmann, C. Becker, and K. Sengstock, Phys. Rev. Lett **107**, 135303 (2011).

[54] A. Brunello, F. Dalfovo, L. Pitaevskii, S. Stringari, and F. Zambelli, Phys. Rev. A **64**, 063614 (2001).

[55] T. A. Corcovilos, S. K. Baur, J. M. Hitchcock, E. J. Mueller, and R. G. Hulet, Phys. Rev. A **81**, 013415 (2010).

[56] The authors thank an anonymous referee for arising this question.